Supporting Information (SI)

† Electronic Supporting Information (ESI) available: 1H-NMR spectra, additional figures, Schemes and Tables

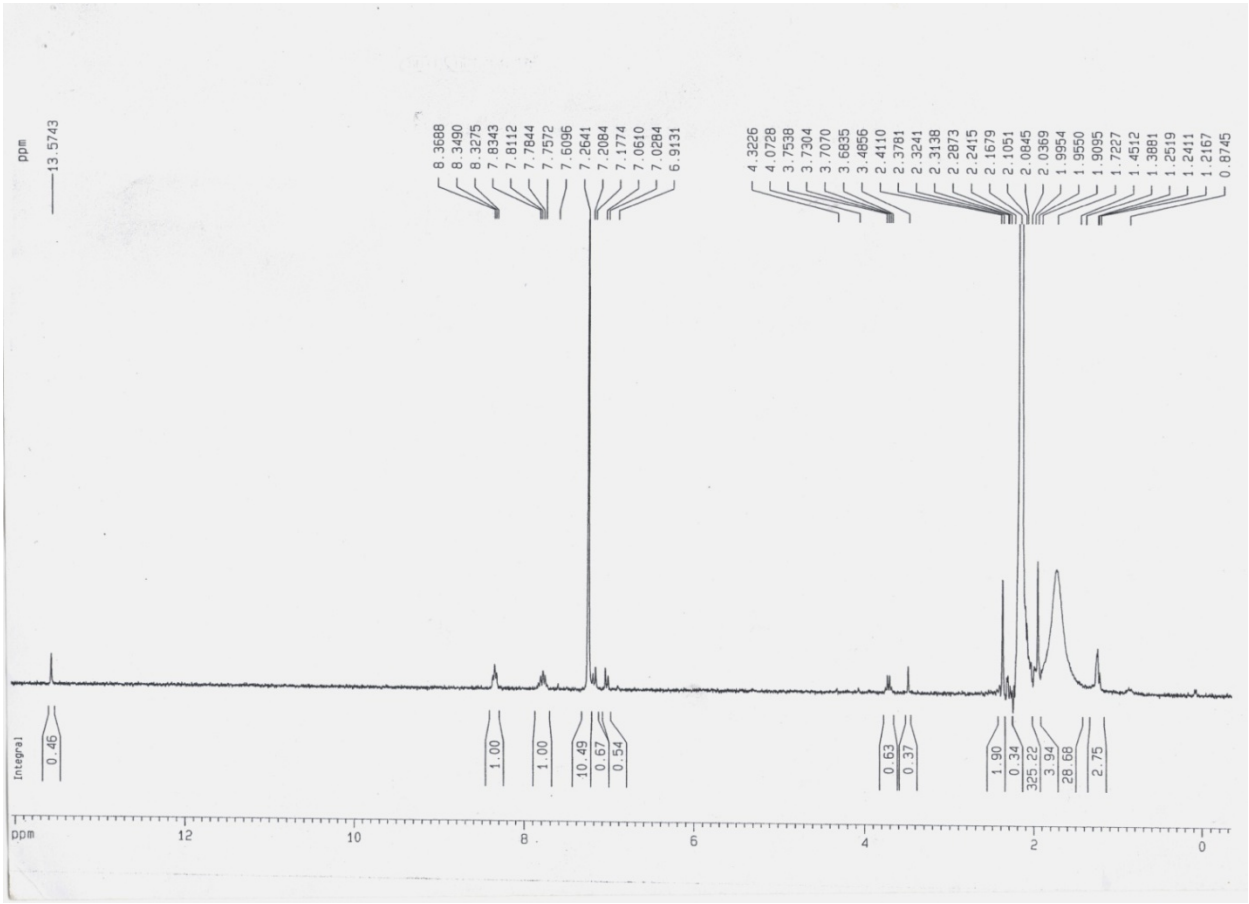

Fig. S1 [1]H NMR Spectra of 1-amino-4-hydroxy-9,10-anthraquinone.

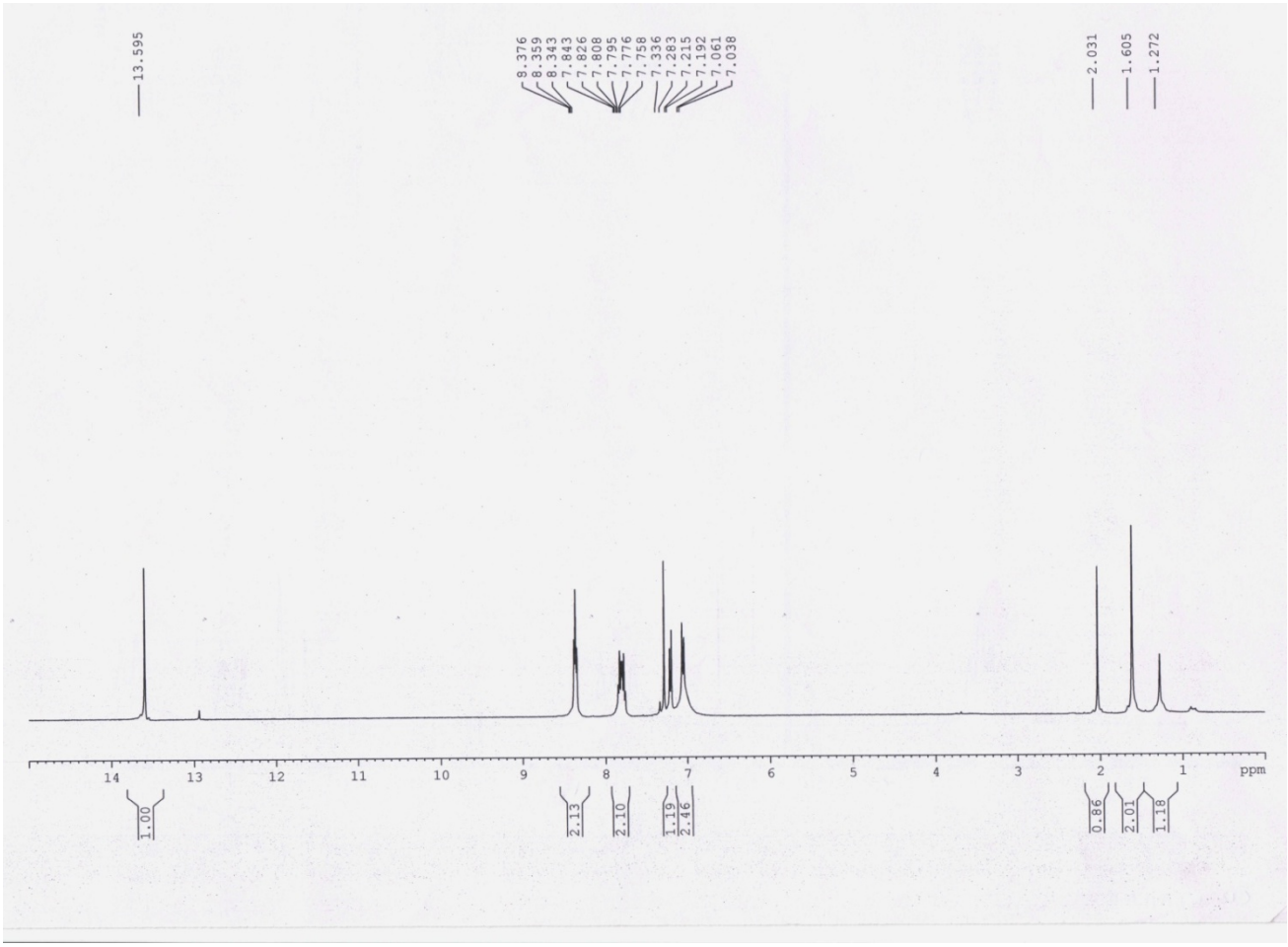

Fig. S2 ^{1}H NMR Spectra of the copper complex of 1-amino-4-hydroxy-9,10-anthraquinone.

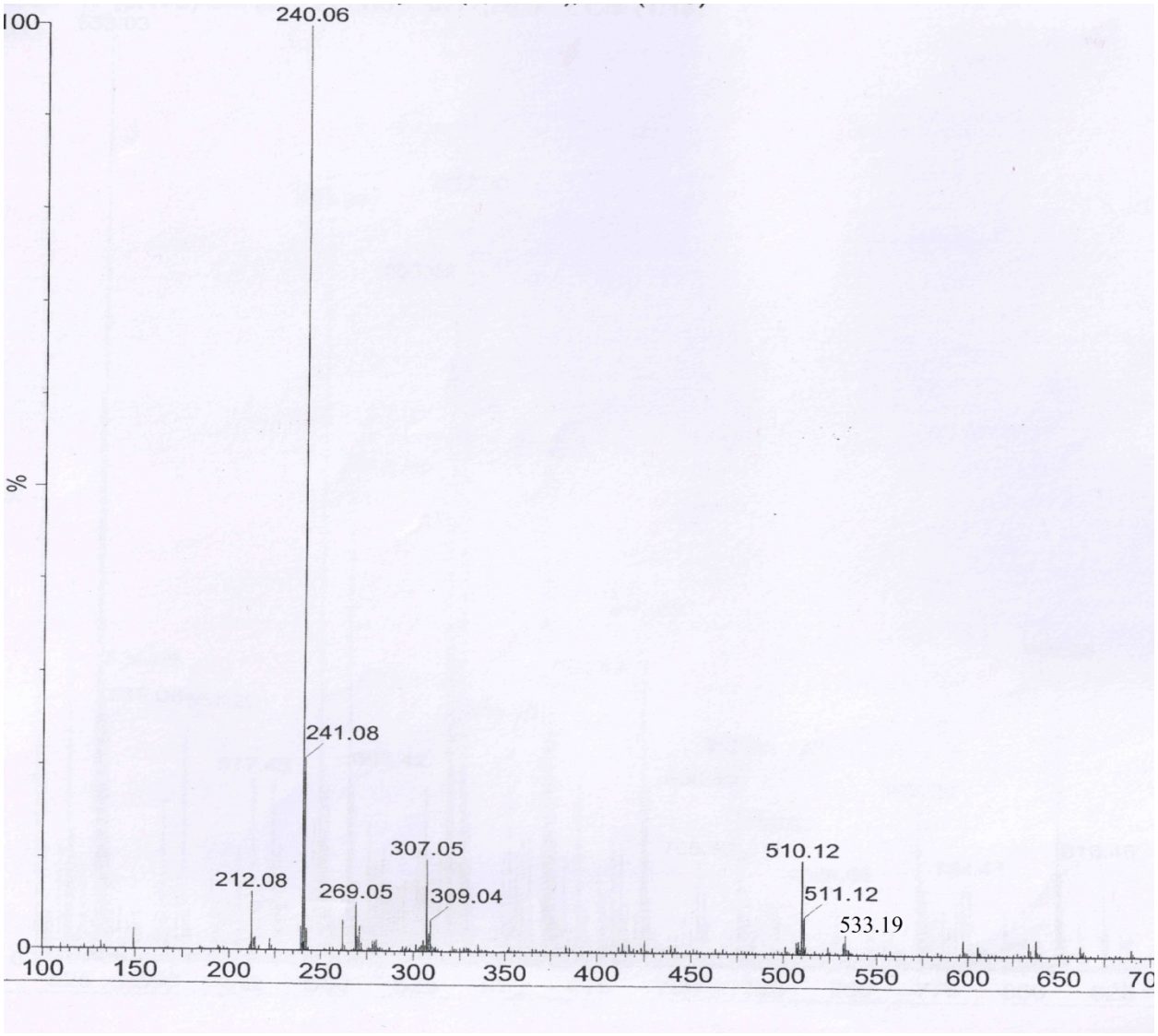

Fig. S3 Mass spectra of the copper complex of 1-amino-4-hydroxy-9,10-anthraquinone.

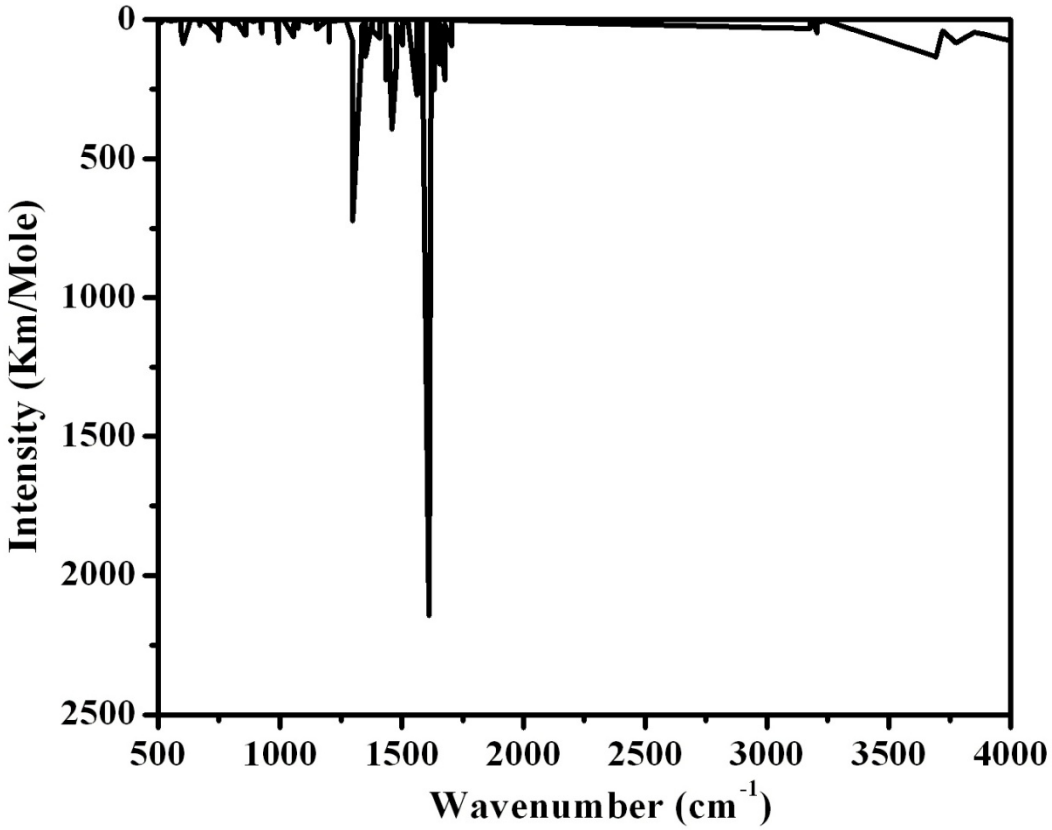

Fig. S4 The theoretical vibrational spectra of copper complex.

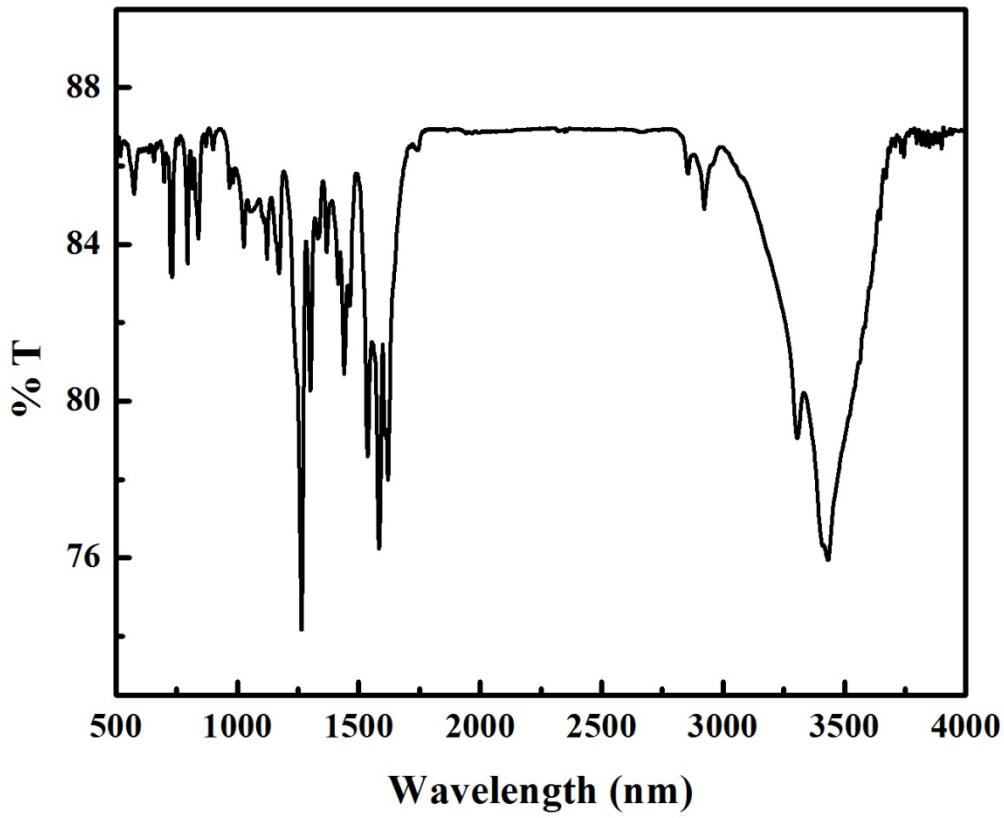

Fig. S5 The experimental vibrational spectra of copper complex.

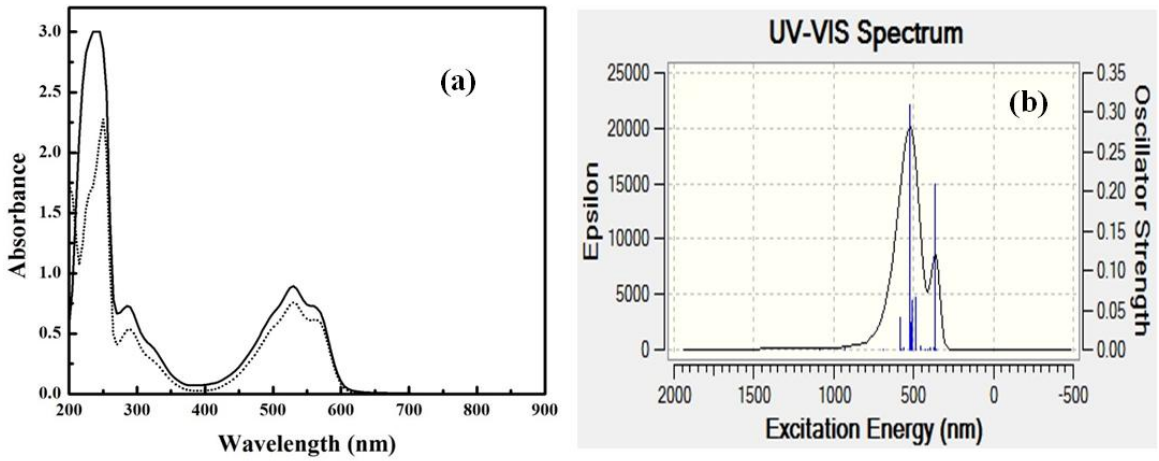

Fig. S6 (a) The UV-Vis spectra of 1-amino-4-hydroxy-9,10-anthraquinone (dotted line) and its copper complex (bold line) in 30% ethanol solution. **(b)** Theoretical UV-Vis spectrum of copper complex.

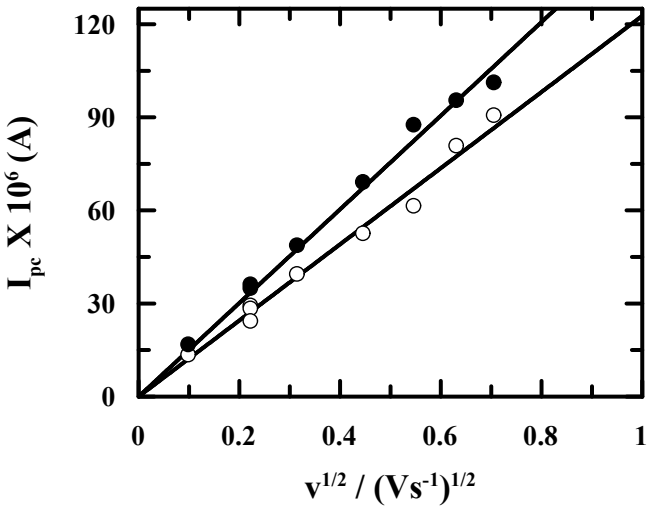

Fig. S7 Plot of the cathodic peak current (Ip_c) with the square root of the scan rate ($\sqrt{v}$) for both the first (o) and second (●) one-electron reductions of the copper complex in anhydrous dimethyl formamide. [CuQ_2] = 10^{-3} M, [TBAB] = 10^{-3} M and temperature = 25^0C.

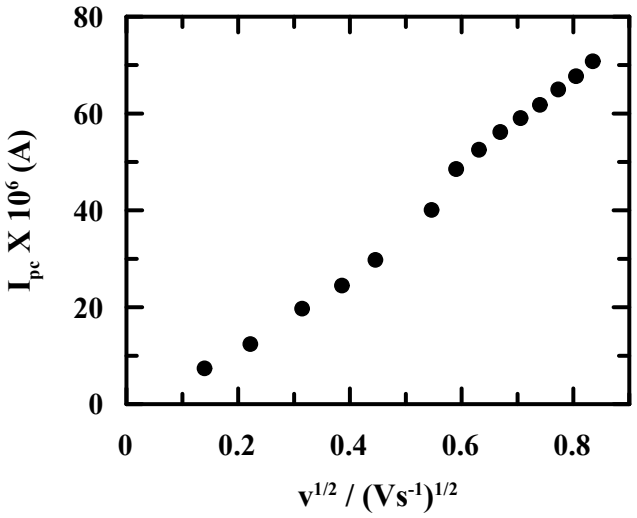

Fig. S8 Plot of the cathodic peak current (Ip_c) with the square root of the scan rate ($\sqrt{v}$) for the reduction of the copper complex in 20% dimethyl formamide. [CuQ_2] = 5×10^{-5} M, [TBAB] = 10^{-3} M and temperature = 25^0C.

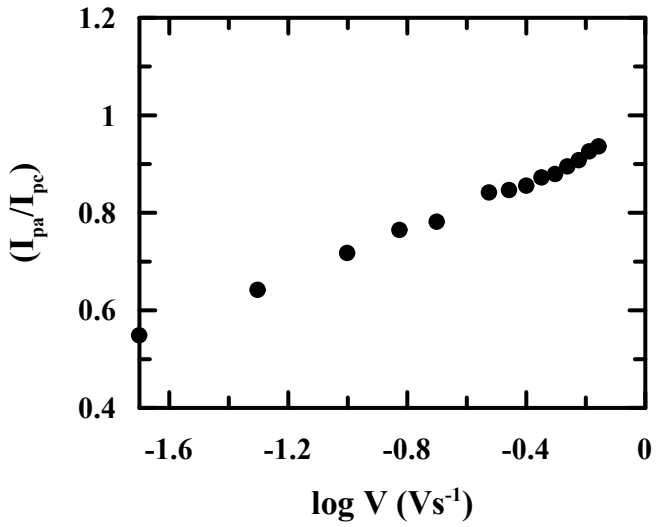

Fig. S9 The plot of the ratio of anodic to cathodic peak current (I_{pa} /I_{pc}) with the logarithm of scan rate (Vs^{-1}) for the reduction of the copper complex in 20% DMF solution.

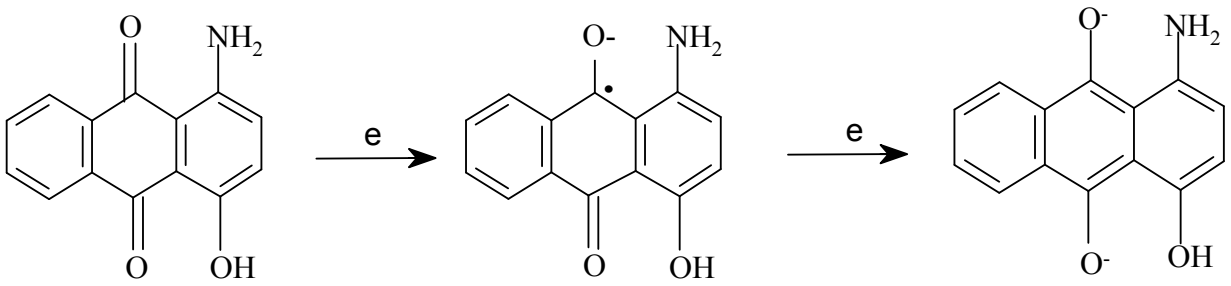

Scheme-S1 Electrochemical reduction of 1-amino-4-hydroxy-9,10-anthraquinone in anhydrous dimethyl formamide.

Table-S1: Comparison of theoretical and experimental IR stretching frequency of the copper complex.

υ_{cal} (cm^{-1})	υ_{scaled} (cm^{-1})	Intensity	PED (%)	Interpretation	υ_{expt} (cm^{-1})
3690	3547	122	S_1(82), S_2(-18) S_3(-82) S_4(18)	υ_{sym} (N_{46}-H_{47}), υ_{asym} (N_{46}-H_{48}) υ_{asym} (N_{50}-H_{51}) υ_{sym}(N_{50}-N_{52})	3430
3469	3334	151	S_3(-16), S_4(75)	υ_{asym} (N_{50}-H_{51}), υ_{sym} ($H_{44}C_{36}$—C_{37})	3410
3238	3112	11.2	S_{14}(92)+ S_8(-92)	υ_{asym} (C_{31}-H_{43}) +υ_{asym} (C_{18}-H_{23})	3205
3207	3082	48	S_{10}(14), S_{12}(79)	υ_{asym} (C_{20}-H_{25}), υ_{asym} (C_{27}-H_{41})	2952
3191	3067	15	S_{10}(69), S_{12}(-14), S_1(15)	υ_{sym} (C_{20}-H_{25}), υ_{asym} (C_{27}-H_{41}), υ_{asym} (N_{46}-H_{47})	2919
3177	3054	33	S_6(89)+ S_{15}(89)	υ_{sym} (C_{27}-C_{28}), υ_{asym} (N_{46}-H_{48})	2849
1704	1638	95	S_{24}(45)+ S_{20}(32), S_{118}(21)	υ_{sym} (O_5-C_{10}), υ_{sym} (O_3-C_{32}), τ (H_{47}-C_{37}-C_{38}-C_{39})	1618
1676	1611	219	S_{29}(-44), S_{62}(23)+ S_{144}(18)	υ_{asym} (C_{14}-C_{20}), β (H_{47}-N_{46}-H_{48}) γ (O49-C8-C15-C12)	1607
1612	1549	2147	S_{35}(-11), S_{62}(-27), S_{17}(11) +S_{59}(25)	υ_{asym} (N_{46}-C_7), β (H_{48}-N_{46}-H_{47}), υ_{asym} (O_{49}-C_{12})+ C=O → Cu	1581
1560	1499	272	S_{23}(-47), S_{75}(11) + S_{143}(34)	υ_{asym} (O_4-C_{36}), β (H_{45}-N_{38}-H_{39}), γ (O53-C29-C34-C33)	1535
1502	1443	93	S_{21}(14), S_{34}(-18), S_{69}(11)	υ_{asym} (C_6-C_{11}), υ_{asym} (C_{26}-C_{31}), β (H_{25}-C_{20} –C_{19}),	1461
1476	1418	172	S_{65}(-10), S_{35}(-10), S_{62}(16), S_{75}(14), S_{64}(-10)	β (H_{21}-C_6-C_{11}), υ_{asym} (N_{46}-C_7), β (H_{48}-N_{46}-H_{47}), β (H_{45}-N_{38}-H_{39}), β (H_{52}-N_{50}-H_{51})	1438

1433	1377	217	S_{42}(-44)	υ_{asym} (C_9-C_{13})	1412
1409	1354	67	S_{75}(23)	β (H_{45}-N_{38}-H_{39})	1366
1349	1296	133	S_{40}(21)	υ_{asym} (C_9-C_{10})	1299
1298	1247	722	S_{47}(-44), S_{48}(-47)	υ_{asym} (C_{12}-C_8), υ_{asym} (C_{33}-C_{34})	1262
1201	1149	89	S_{70}(42), S_{70}(13), S_{34}(-12), S_{28}(23)	β (H_{40}-C_{26}–C_{31}), β (H_{40}-C_{26}–C_{31}), υ_{asym} (C_{26}-C_{31}), υ_{asym} (C_{30}-C_{31})	1169
1149	1104	34	S_{61}(22)	β (H_{48}-N_{46}-H_{47})	1123
991	952	85	S_{26}(-20), S_{40}(-14)	υ_{asym} (C_{20}-C_{19}), υ_{asym} (C_{10}-C_9)	1024
922	886	47	S_{58}(-12), S_{88}(14)	β (C_{33}-C_{34}–C_{39}), β (C_{19}-C_{18}–C_{16})	839
860	826	57	S_{119}(74)	τ (H_{45}-C_{38}-C_{39}-N_{50})	814
748	719	75	S_{115}(-25)	τ (H_{41}-C_{27}-C_{28}-C_{29})	794
673	646	22	S_{53}(15)+S_{56}(20)	β (C_{15}-C_{16}–C_{18}), β (C_{34}-C_{39}–C_{38})	726
604	580	86	S_{51}(-10), S_{90}(12), S_{52}(-12)	υ_{asym} (Cu_1-O_4), β (C_{31}-C_{26}–C_{27}), υ_{asym} (Cu_1-O_5)	656
595	572	38	S_{151}(34), S_{152}(49), S_{52}(12)	τ (C_{11}-C_9-O_5-C_{10}), τ (C_{37}-C_{35}-O_4-C_{36}), υ_{sym} (Cu_1-O_5)	571

[+ sign is used to indicate a combination mode]

Table-S2: Major contributions of Atomic Orbitals to the Molecular Orbitals involved in UV-visible transitions [a]

Molecular orbitals	**% Contribution of atomic orbitals[b]**
$(HOMO-2)_{\alpha}$	Cu1-d=22 O5-p=15 O4-p=15 O2-p=12 O3-p=12
$(HOMO-1)_{\alpha}$	N46-p=9 N50-p=9
$(HOMO)_{\alpha}$	N46-p=9
$(LUMO)_{\alpha}$	C32-p=7 C36-p=7 C10-p=5 C13-p=5
$(LUMO+1)_{\alpha}$	C13-p=7
$(LUMO+2)_{\alpha}$	C16-p=9
$(HOMO-3)_{\beta}$	O49-p=32 O53-p=32
$(HOMO-2)_{\beta}$	O53-p=18 O49-p=18
$(HOMO-1)_{\beta}$	N50-p=9
$(HOMO)_{\beta}$	N46-p=8
$(LUMO)_{\beta}$	C32-p=7 C14-p=7 C15-p=7 C34-p=7 C35-p=7
$(LUMO+1)_{\beta}$	C13-p=6

[a] Only atomic orbitals having 5% or more contributions are listed;
. [b] Atom numbering scheme as in Figure 5.